Available online at www.pelagiaresearchlibrary.com

Pelagia Research Library

Advances in Applied Science Research, 2012, 3 (1):452-461

ISSN: 0976-8610
CODEN (USA): AASRFC

Peristaltic flow of a Williamson fluid in an inclined planar channel under the effect of a magnetic field

B. Jayarami Reddy[a], M. V. Subba Reddy[b], C. Nadhamuni Reddy[c] and P. Yogeswar Reddy[d]

[a]Department of Civil Engineering, YSR Engineering College of Yogi Vemana University, Proddatur, A.P., India
[b]Department of Computer Science & Engineering, Sri Venkatesa Perumal College of Engineering &Technology, Puttur, A.P, India
[c]Department of Mechanical Engineering, Sri Venkatesa Perumal College of Engineering &Technology, Puttur, A.P., India
[d]Department of Mathematics, Vemana Institute of Technology, Bangalore, India

---

ABSTRACT

In this paper, the MHD peristaltic flow of a Williamson fluid in a planar channel, under the assumptions of long wavelength is investigated. The flow is investigated in a wave frame of reference moving with velocity of the wave. The perturbation series in the Weissenberg number was used to obtain explicit forms for velocity field and pressure gradient. The effects of Weissenberg number and Hartmann number on the pumping characteristics are discussed through graphs in detail.

Keywords: Hartmann number; peristaltic flow; Reynolds number; Williamson fluid.

INTRODUCTION

Peristalsis is an important mechanism generated by the propagation of waves along the walls of a channel or tube. It occurs in the gastrointestinal, urinary, reproductive tracts and many other glandular ducts in a living body.

Most of the studies on the topic have been carried out for the Newtonian fluid for physiological peristalsis including the flow of blood in arterioles. But such a model cannot be suitable for blood flow unless the non-Newtonian nature of the fluid is included in it. The non-Newtonian peristaltic flow using a constitutive equation for a second order fluid has been investigated by Siddiqui et al. [7] for a planar channel and by Siddiqui and Schwarz [9] for an axisymmetric tube. They have performed a perturbation analysis with a wave number, including curvature and inertia effects and have determined range of validity of their perturbation solutions. The effects of third order fluid on peristaltic transport in a planar channel were studied by Siddiqui et al. [8] and the corresponding axisymmetric tube results were obtained by Hayat et al. [2]. Haroun [1] studied peristaltic transport of third order fluid in an asymmetric channel. Subba Reddy et al. [11] have studied the peristaltic flow of a power-law fluid in an asymmetric channel. Peristaltic motion of a Williamson fluid in an asymmetric channel was studied by Nadeem and Akram [6].

It is now well known that blood behaves like a magnetohydrodynamic (MHD) fluid (Stud et al. [10]). Blood is a suspension of cells in plasma. It is a biomagnetic fluid, due to the complex integration of the intercellular protein, cell membrane and the hemoglobin, a form of iron oxide, which is present at a uniquely high concentration in the mature red cells, while its magnetic property is influenced by factors such as the state of oxygenation. The consideration of blood as a MHD fluid helps in controlling blood pressure and has potential for therapeutic use in the diseases of heart and blood vessels (Mekheimer [5]). Peristaltic transport to a MHD third order fluid in a circular cylindrical tube was investigated by Hayat and Ali [3]. Hayat et al. [4] have investigated peristaltic transport of a third order fluid under the effect of a magnetic field. Recently, Subba Reddy et al. [12] have studied the peristaltic transport of Williamson fluid in a channel under the effect of a magnetic field.

In view of these, we modeled the MHD peristaltic flow of a Williamson fluid in an inclined planar channel, under the assumptions of long wavelength. The flow is investigated in a wave frame of reference moving with velocity of the wave. The perturbation series in the Weissenberg number was used to obtain explicit forms for velocity field and pressure gradient. The effects of various emerging parameters on the pumping characteristics are studied in detail with the help of graphs.

2. Mathematical Formulation

We consider the peristaltic flow of a Williamson fluid in a two-dimensional symmetric channel of width $2a$. The channel walls are inclined at an angle θ to the horizontal. The fluid is conducting while the channel walls are non-conducting. The flow is generated by sinusoidal wave trains propagating with constant speed 'c' along the channel walls. Fig. 1 shows the schematic diagram of the channel.

The wall deformation is given by

$$Y = \pm H(X,t) = \pm a \pm b\cos\frac{2\pi}{\lambda}(X - ct), \qquad (2.1)$$

where b is the amplitude of the wave, λ - the wave length and X and Y - the rectangular co-ordinates with X measured along the axis of the channel and Y perpendicular to X. Let (U,V) be the velocity components in fixed frame of reference (X,Y).

The flow is unsteady in the laboratory frame (X,Y). However, in a co-ordinate system moving with the propagation velocity c (wave frame (x, y)), the boundary shape is stationary. The transformation from fixed frame to wave frame is given by

$$x = X - ct, y = Y, u = U - c, v = V \qquad (2.2)$$

where (u,v) and (U,V) are velocity components in the wave and laboratory frames respectively.

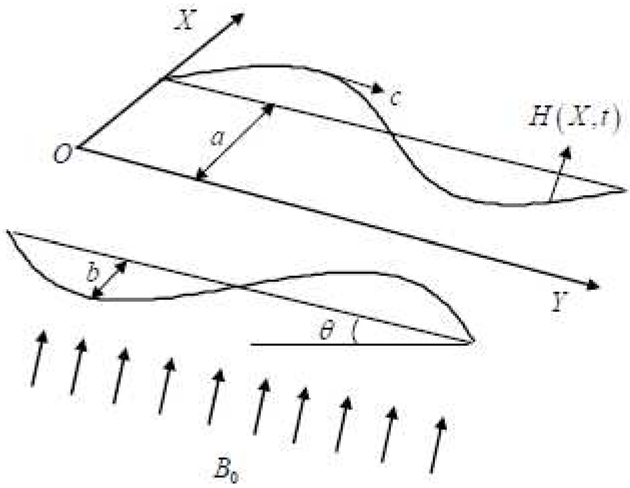

Fig.1 The physical model

The constitutive equation for a Williamson fluid (given in Bird et al. 1977) is

$$\tau = -\left[\eta_\infty + (\eta_0 + \eta_\infty)(1 - \Gamma\dot{\gamma})^{-1}\right]\dot{\gamma} \qquad (2.3)$$

Where τ is the extra stress tensor, η_∞ is the infinite shear rate, viscosity η_o is the zero shear rate viscosity, Γ is the time constant and $\dot{\gamma}$ is defined as

$$\dot{\gamma} = \sqrt{\frac{1}{2}\sum_i \sum_j \dot{\gamma}_{ij}\dot{\gamma}_{ji}} = \sqrt{\frac{1}{2}\pi} \tag{2.4}$$

where π is the second invariant stress tensor. We consider in the constitutive equation (2.3) the case for which $\eta_\infty = 0$ and $\Gamma\dot{\gamma} < 1$ so we can write.

$$\tau = -\eta_0\left(1 + \Gamma\dot{\gamma}\right)\dot{\gamma} \tag{2.5}$$

The above model reduces to Newtonian for $\Gamma = 0$

The equations governing the flow in the wave frame of reference are

$$\frac{\partial u}{\partial x} + \frac{\partial v}{\partial y} = 0 \tag{2.6}$$

$$\rho\left(u\frac{\partial u}{\partial x} + v\frac{\partial u}{\partial y}\right) = -\frac{\partial p}{\partial x} - \frac{\partial \tau_{xx}}{\partial x} - \frac{\partial \tau_{yx}}{\partial y} - \sigma B_0^2\left(u + c\right) + \rho g \sin\theta \tag{2.7}$$

$$\rho\left(u\frac{\partial v}{\partial x} + v\frac{\partial u}{\partial y}\right) = -\frac{\partial p}{\partial y} - \frac{\partial \tau_{xy}}{\partial x} - \frac{\partial \tau_{yy}}{\partial y} - \rho g \cos\theta \tag{2.8}$$

where ρ is the density, B_0 is the magnetic field strength, σ is the electrical conductivity and k is the permeability of the porous medium.

The boundary conditions are

$$u = -c \quad \text{at} \quad y = H = a + b\cos\left(\frac{2\pi}{\lambda}x\right) \tag{2.9}$$

$$\frac{\partial u}{\partial y} = 0 \quad \text{at} \quad y = 0 \tag{2.10}$$

Introducing the non-dimensional variables defined by

$$\bar{x} = \frac{x}{\lambda},\ \bar{y} = \frac{y}{a},\ \bar{u} = \frac{u}{c},\ \bar{v} = \frac{v}{c\delta},\ \delta = \frac{a}{\lambda},\ \bar{p} = \frac{pa^2}{\eta_0 c\lambda},$$
$$h = \frac{H}{a},\ \bar{t} = \frac{ct}{\lambda},\ \tau_{xx} = \frac{\lambda}{\eta_0 c}\tau_{xx},\ \bar{\tau}_{xy} = \frac{a}{\eta_0 c}\tau_{xy},\ \tau_{yy} = \frac{\lambda}{\eta_0 c}\tau_{yy},$$
$$\mathrm{R}_e = \frac{\rho ac}{\eta_0},\ We = \frac{\Gamma c}{a},\ \bar{\dot{\gamma}} = \frac{\dot{\gamma}a}{c},\ \bar{q} = \frac{q}{ac} \tag{2.11}$$

into the Equations (2.5) - (2.8), reduce to (after dropping the bars)

$$\frac{\partial u}{\partial x} + \frac{\partial v}{\partial y} = 0 \tag{2.12}$$

$$\mathrm{Re}\,\delta\left(u\frac{\partial u}{\partial x}+v\frac{\partial u}{\partial y}\right)=-\frac{\partial p}{\partial x}-\delta^2\frac{\partial \tau_{xx}}{\partial x}-\frac{\partial \tau_{xy}}{\partial y}-M^2(u+1)+\frac{\mathrm{Re}}{Fr}\sin\theta \qquad (2.13)$$

$$\mathrm{Re}\,\delta^3\left(u\frac{\partial v}{\partial x}+v\frac{\partial v}{\partial y}\right)=-\frac{\partial p}{\partial y}-\delta^2\frac{\partial \tau_{xy}}{\partial y}-\delta\frac{\partial \tau_{yy}}{\partial y}-\frac{Re}{Fr}\delta\cos\theta \qquad (2.14)$$

where

$$\tau_{xx}=-2\left[1+We\,\dot\gamma\right]\frac{\partial u}{\partial x},\qquad \tau_{xy}=-\left[1+We\,\dot\gamma\right]\left(\frac{\partial u}{\partial y}+\delta^2\frac{\partial v}{\partial x}\right),\qquad \tau_{yy}=-2\delta\left[1+We\,\dot\gamma\right]\frac{\partial v}{\partial y},$$

$\dot\gamma=\left[2\delta^2\left(\frac{\partial u}{\partial x}\right)^2+\left(\frac{\partial u}{\partial y}+\delta^2\frac{\partial v}{\partial x}\right)^2+2\delta^2\left(\frac{\partial v}{\partial y}\right)^2\right]^{\frac{1}{2}}$, $M^2=aB_0\sqrt{\frac{\sigma}{\eta_0}}$ is the Hartmann numberand

$Fr=\frac{c^2}{ag}$ is the Froude number.

Under the assumption of long wavelength approximation ($\delta \ll 1$), the Eqs. (2.13) and (2.14) become

$$\frac{\partial p}{\partial x}=\frac{\partial}{\partial y}\left\{\left[1+We\frac{\partial u}{\partial y}\right]\frac{\partial u}{\partial y}\right\}-M^2(u+1)+\frac{\mathrm{Re}}{Fr}\sin\theta \qquad (2.15)$$

$$\frac{\partial p}{\partial y}=0 \qquad (2.16)$$

From Eq. (2.13) and (2.14), we get

$$\frac{dp}{dx}=\frac{\partial^2 u}{\partial y^2}+We\frac{\partial}{\partial y}\left[\left(\frac{\partial u}{\partial y}\right)^2\right]-M^2(u+1)+\frac{\mathrm{Re}}{Fr}\sin\theta \qquad (2.17)$$

The corresponding non-dimensional boundary conditions are

$$u=-1 \quad \text{at} \quad y=h=1+\phi\cos(2\pi x) \qquad (2.18)$$

$$\frac{\partial u}{\partial y}=0 \quad \text{at} \quad y=0 \qquad (2.19)$$

The volume flow rate q in a wave frame of reference is given by

$$q=\int_0^h u\,dy\,. \qquad (2.20)$$

The instantaneous flow Q(X,t) in the laboratory frame is

$$Q(X,t)=\int_0^h U\,dY=\int_0^h (u+1)\,dy=q+h \qquad (2.21)$$

The time averaged volume flow rate $\overline{Q}$ over one period $T\left(=\frac{\lambda}{c}\right)$ of the peristaltic wave is given by

$$\overline{Q} = \frac{1}{T}\int_0^T Q dt = q + 1 \tag{2.22}$$

3. Solution

Since Eq. (2.17) is a non-liner differential equation, it is not possible to obtain closed form solution. Therefore we employ regular perturbation to find the solution.

For perturbation solution, we expend u, p and q as follows

$$u = u_0 + We\, u_1 + O\left(We^2\right) \tag{3.1}$$

$$\frac{dp}{dx} = \frac{dp_0}{dx} + We\frac{dp_1}{dx} + O\left(We^2\right) \tag{3.2}$$

$$q = q_0 + We\, q_1 + O\left(We^2\right) \tag{3.3}$$

Substituting these equations in the Eqs. (2.15) - (2.17), we obtain

3.1. System of order We^0

$$\frac{dp_0}{dx} = \frac{\partial^2 u_0}{\partial y^2} - M^2\left(u_0 + 1\right) \tag{3.4}$$

and the respective boundary conditions are

$$u_o = -1 \quad \text{at} \quad y = h \tag{3.5}$$

$$\frac{\partial u_0}{\partial y} = 0 \quad \text{at} \quad y = 0 \tag{3.6}$$

3.2. System of order We^1

$$\frac{dp_1}{dx} = \frac{\partial^2 u_1}{\partial y^2} + \frac{\partial}{\partial y}\left[\left(\frac{\partial u_o}{\partial y}\right)^2\right] - M^2 u_1 \tag{3.7}$$

and the respective boundary conditions are

$$u_1 = 0 \quad \text{at} \quad y = h \tag{3.8}$$

$$\frac{\partial u_1}{\partial y} = 0 \quad \text{at} \quad y = 0 \tag{3.9}$$

3.3 Solution for system of order We^0

Solving Eq. (3.4) using the boundary conditions (3.5) and (3.6), we obtain

$$u_0 = \frac{1}{M^2}\left(\frac{dp_0}{dx} - \frac{\mathrm{Re}}{Fr}\sin\theta\right)\left[\frac{\cosh My}{\cosh Mh} - 1\right] - 1 \tag{3.10}$$

The volume flow rate q_0 is given by

$$q_0 = \frac{1}{M^2}\left(\frac{dp_0}{dx} - \frac{\mathrm{Re}}{Fr}\sin\theta\right)\left[\left(\frac{\sinh Mh - Mh\cosh Mh}{M\cosh Mh}\right) - h\right] \tag{3.11}$$

From Eq. (3.11), we have

$$\frac{dp_0}{dx} = \frac{(q_0+h)M^3\cosh Mh}{\sinh Mh - Mh\cosh Mh} + \frac{\mathrm{Re}}{Fr}\sin\theta \tag{3.12}$$

3.4 Solution for system of order We^1

Substituting Equation (3.10) in the Eq. (3.7) and solving the Eq. (3.7), using the boundary conditions (3.8) and (3.9), we obtain

$$u_1 = \frac{1}{M^2}\frac{dp_1}{dx}\left[\frac{\cosh My}{\cosh Mh} - 1\right] + \frac{2}{3}\frac{\left(\frac{dp_0}{dx} - \frac{\mathrm{Re}}{Fr}\sin\theta\right)^2}{M^3\cosh^2 Mh}\left[\begin{array}{l} 2\sinh My - \sinh 2My + \\ 2(\sinh Mh - \tanh Mh)\cosh My \end{array}\right] \tag{3.13}$$

The volume flow rate q_1 is given by

$$\begin{aligned} q_1 = {} & \frac{1}{M^3}\frac{dp_1}{dx}\left[\frac{\sinh Mh - hM\cosh Mh}{\cosh Mh}\right] \\ & + \frac{2}{3}\frac{\left(\frac{dp_0}{dx} - \frac{\mathrm{Re}}{Fr}\sin\theta\right)^2}{M^3\cosh^2 Mh}\left\{\begin{array}{l} \frac{2}{M}(\cosh Mh - 1) - \frac{[\cosh 2Mh - 1]}{2M} + \\ \frac{2}{M}(\sinh\ Mh - \tanh\ Mh)\sinh\ Mh \end{array}\right\} \end{aligned} \tag{3.14}$$

From Eq. (3.14) and (3.12), we have

$$\frac{dp_1}{dx} = \frac{q_1 M^3\cosh Mh}{\sinh Mh - Mh\cosh Mh} - \frac{2}{3}\frac{\Psi(q_o+h)^2 M^6\cosh Mh}{[\sinh Mh - Mh\cosh Mh]^3} \tag{3.15}$$

where $\Psi = \frac{2}{M}(\cosh Mh - 1) + \frac{2}{M}(\sinh Mh - \tanh Mh)\sinh Mh - \frac{1}{2M}(\cosh 2Mh - 1)$

Substituting Equations (3.12) and (3.15) into the Equation (3.2), we get

$$\frac{dp}{dx} = \frac{(q+h)M^3\cosh Mh}{\sinh Mh - Mh\cosh Mh} - We\frac{2\Psi(q+h)^2 M^6\cosh Mh}{3[\sinh Mh - Mh\cosh Mh]^3} + \frac{\mathrm{Re}}{Fr}\sin\theta \tag{3.16}$$

The dimensionless pressure rise per one wavelength in the wave frame are defined, respectively as

$$\Delta p = \int_0^1 \frac{dp}{dx}dx \tag{3.17}$$

RESULTS AND DISCUSSION

Fig. 2 shows the variation of pressure rise Δp with $\overline{Q}$ for different values of Weissenberg number We with $\phi = 0.5, \theta = \frac{\pi}{4}$, $Fr = 2, \mathrm{Re} = 10$ and $M = 1$. It is observed that, $\overline{Q}$ increases with an increase in We in all the three regions; pumping region $(\Delta p > 0)$, free-pumping region $(\Delta p = 0)$ and co-pumping region $(\Delta p = 0)$.

The variation of pressure rise Δp with $\overline{Q}$ for different values of Hartmann number M with $\phi = 0.5, \mathrm{Re} = 10,\ \theta = \frac{\pi}{4}, Fr = 2$ and $We = 0.01$ is shown in Fig. 3. It is observed that, any two pumping curves intersect at a point in the first quadrant. To the left of this point $\overline{Q}$ increases and to the right of this point the $\overline{Q}$ on increasing M. Fig. 4 illustrates the variation of pressure rise Δp with $\overline{Q}$ for different values of amplitude ratio ϕ with $M = 1, \mathrm{Re} = 10,\ \theta = \frac{\pi}{4}, Fr = 2$ and $We = 0.01$. It is observed that, the $\overline{Q}$ increases with increasing ϕ in the pumping region. While it decreases with increasing ϕ in both free-pumping and co-pumping regions.

The variation of pressure rise Δp with $\overline{Q}$ for different values of inclination angle θ with $M = 1, \mathrm{Re} = 10,\ \phi = 0.5, Fr = 2$ and $We = 0.01$ is shown in Fig. 5. It is observed that, the $\overline{Q}$ increases on increasing θ in all the three regions. Fig. 6 depicts the variation of pressure rise Δp with $\overline{Q}$ for different values of Froude number Fr with $M = 1, \mathrm{Re} = 10,\ \phi = 0.5, \theta = \frac{\pi}{4}$ and $We = 0.01$. It is found that, the $\overline{Q}$ decreases with increasing Fr in all the three regions.

The variation of pressure rise Δp with $\overline{Q}$ for different values of Reynolds number θ with $M = 1, \theta = \frac{\pi}{4},\ \phi = 0.5, Fr = 2$ and $We = 0.01$ is shown in Fig. 7. It is found that, the $\overline{Q}$ increases with increasing Re in all the three regions.

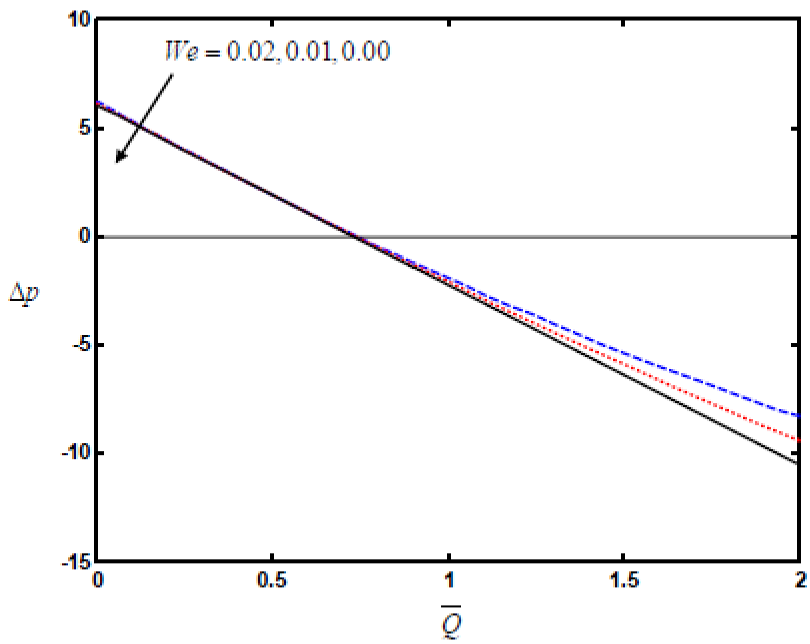

Fig. 2. The variation of pressure rise Δp with $\overline{Q}$ for different values of Weissenberg number We with $\phi = 0.7, \theta = \frac{\pi}{4},\ Fr = 2, \mathrm{Re} = 10$ and $M = 1$.

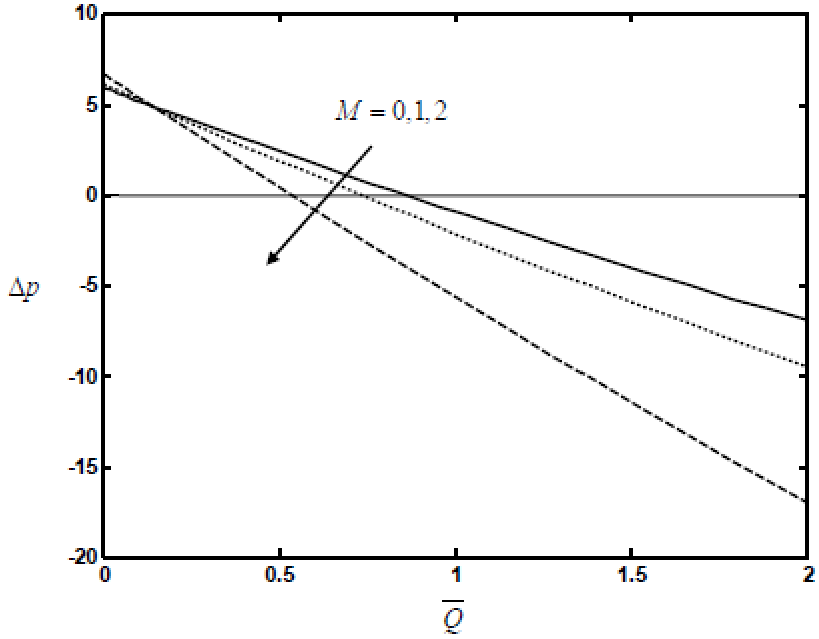

Fig. 3. The variation of pressure rise Δp with $\overline{Q}$ for different values of Hartmann number M with $\phi = 0.5, \mathrm{Re} = 10,\ \theta = \frac{\pi}{4}, Fr = 2$ and $We = 0.01$.

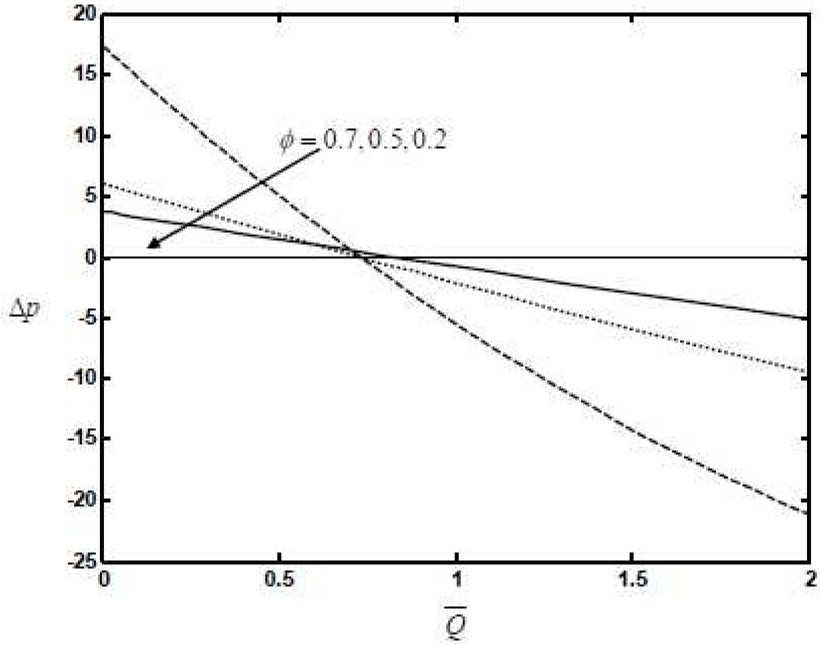

Fig. 4. The variation of pressure rise Δp with $\overline{Q}$ for different values of amplitude ratio ϕ with $M = 1, \mathrm{Re} = 10,\ \theta = \frac{\pi}{4}, Fr = 2$ and $We = 0.01$.

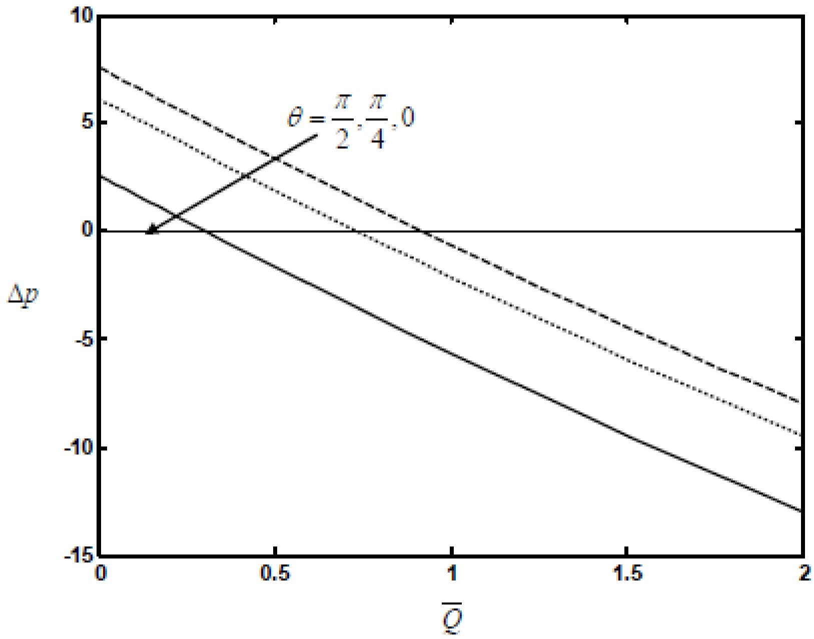

Fig. 5. The variation of pressure rise Δp **with** $\overline{Q}$ **for different values of inclination angle** θ **with** $M = 1, \mathrm{Re} = 10, \ \phi = 0.5, Fr = 2$ **and** $We = 0.01$.

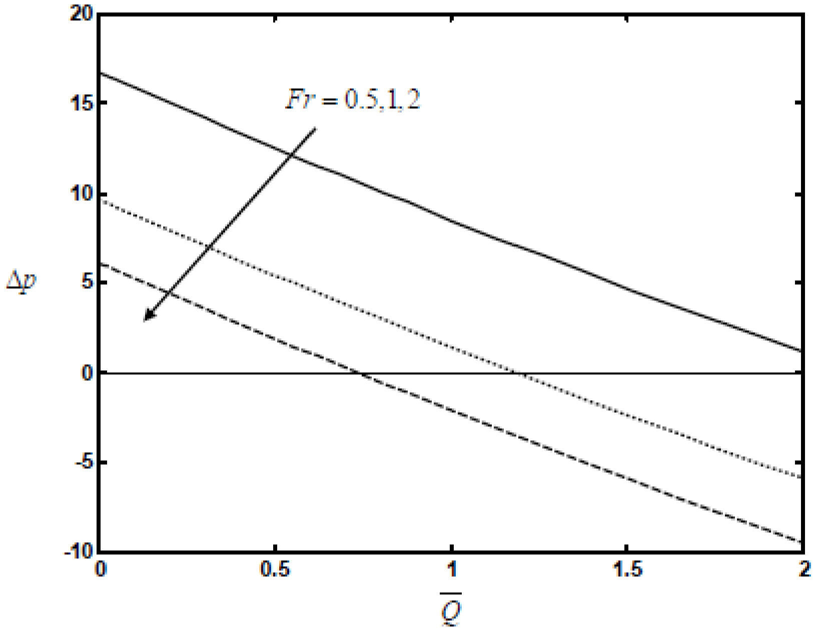

Fig. 6. The variation of pressure rise Δp **with** $\overline{Q}$ **for different values of Froude number** Fr **with** $M = 1, \mathrm{Re} = 10, \ \phi = 0.5, \theta = \frac{\pi}{4}$ **and** $We = 0.01$.

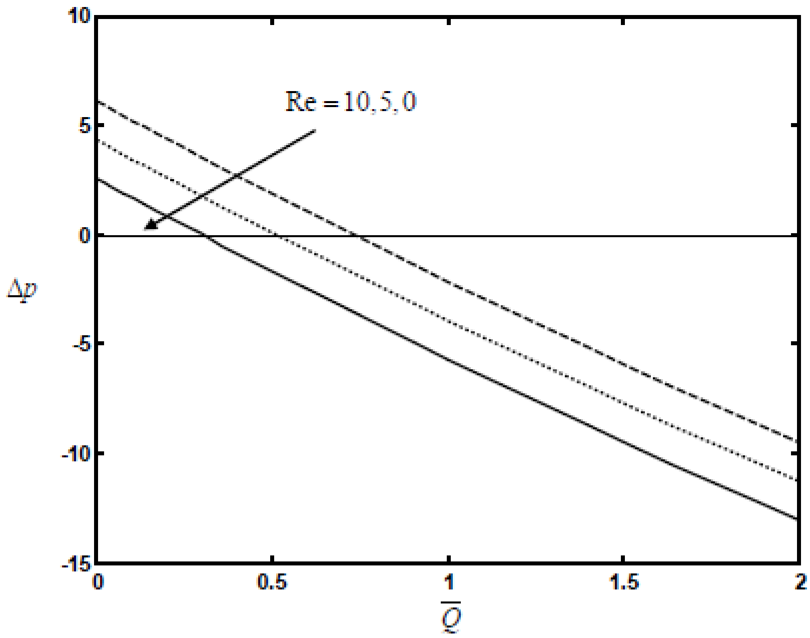

Fig. 7. The variation of pressure rise Δp with $\overline{Q}$ for different values of Reynolds number θ with $M = 1, \theta = \frac{\pi}{4}, \phi = 0.5, Fr = 2$ and $We = 0.01$.

CONCLUSION

In this paper, we investigated the MHD peristaltic flow of a Williamson fluid in a planar channel under the assumptions of long wavelength. The flow is investigated in a wave frame of reference moving with velocity of the wave. The perturbation series in the Weissenberg number was used to obtain explicit forms for velocity field and pressure gradient. It is observed that, in the pumping region, the time-averaged volume flow rate $\overline{Q}$ increases with increasing Weissenberg number We, Hartmann number M, amplitude ratio ϕ, inclination angle θ or Reynolds number Re, while it decreases with increasing Froude number Fr.

REFERENCES

[1] Haroun, M.A. *Comm. Non linear sic. Number. Simul*., 12 (**2007**), 1464 -1480.
[2] Hayat, T., Wang, Y., Siddiqui, A.M., Hutter, K. and Asghar, S. *Math. Models & Methods in Appl. Sci*., 12(**2002**), 1691-1706.
[3] Hayat, T and Ali, N. *Physica A: Statistical Mechanics and its Applications*, 370(**2006**), 225-239.
[4] Hayat, T., Afsar, A., Khan, M. and Asghar, S. *Computers and Mathematics with Applications*, 53(**2007**), 1074-1087.
[5] Mekheimer, KH.S. *Appl. Math. Comput*, 153 (**2004**), 763-777.
[6] Nadeem, S. and Akram, S. *Comm. Non linear sic. Numer. Simul*., 15 (**2010**), 1705–1716
[7] Siddiqui, A.M., Provost, A. and Schwarz, W.H. *Rheol.Acta*, 30(**1991**), 249-262.
[8] Siddiqui, A.M., Provost, A. and Schwarz, W.H., *Rheol.Acta*, 32(**1993**), 47-56
[9] Siddiqui, A.M. and Schwarz, W.H. *J. Non-Newtonian Fluid Mech*., 53(**1994**), 257-284.
[10] Stud, V.K., Sekhon, G.S. and Mishra, R.K. *Bull. Math. Biol*. 39(**1977**), 385-390.
[11] Subba Reddy, M.V., Ramachandra Rao, A. and Sreenadh, S. *Int. J. Non-Linear Mech*., 42 (**2007**), 1153-1161.
[12] Subba Reddy, M. V., Jayarami Reddy, B. and Prasanth Reddy, D. *International Journal of Fluid Mechanics*, 3(1)(**2011**), 89-109.